JOURNAL OF GEOPHYSICAL RESEARCH, VOL. 114, C05017, doi:10.1029/2008JC004955, 2009

On the characteristics of Circumpolar Deep Water intrusions to the west Antarctic Peninsula Continental Shelf

C. Moffat,[1,2] B. Owens,[1] and R. C. Beardsley[1]

Received 10 June 2008; revised 25 November 2008; accepted 25 February 2009; published 19 May 2009.

[1] Hydrographic and current velocity observations collected from March 2001 to February 2003 on the west Antarctic Peninsula shelf as part of the Southern Ocean Global Ecosystems Dynamics program are used to characterize intrusions of Upper Circumpolar Deep Water (UCDW) and Lower Circumpolar Deep Water (LCDW) onto the shelf and Marguerite Bay. UCDW is found on the middle and outer shelf along Marguerite Trough, which connects the shelf break to Marguerite Bay, and at another location farther south. UCDW intrudes in the form of frequent (four per month) and small horizontal scales (≈4 km) warm eddy-like structures with maximum vertical scales of a few hundred meters. However, no evidence of UCDW intrusions was found in Marguerite Bay. LCDW was found in several deep depressions connected to the shelf break, including Marguerite Trough, forming a tongue of relatively dense water 95 m thick (on average) that reaches into Marguerite Bay through Marguerite Trough. A steady advective-diffusive balance for the LCDW intrusion is used to make an estimation of the average upwelling rate and diffusivity in the deep layer within Marguerite Trough, which suggest the LCDW layer is renewed approximately every six weeks.

Citation: Moffat, C., B. Owens, and R. C. Beardsley (2009), On the characteristics of Circumpolar Deep Water intrusions to the west Antarctic Peninsula Continental Shelf, *J. Geophys. Res.*, *114*, C05017, doi:10.1029/2008JC004955.

1. Introduction

[2] Early studies of the western Antarctic Peninsula (wAP) shelf (Figure 1) revealed a complex hydrographic structure with a strong seasonal cycle. The surface layer is occupied by Antarctic Surface Water (AASW), a relatively fresh and cold water mass that is usually found all around the Antarctic continent. During the late fall and winter, the surface mixed layer is deepened by surface cooling and by brine rejection because of the formation of a seasonal ice cover. The resulting mixed layer is roughly at the freezing point and reaches a depth of about 100 m. As the air temperature increases at the end of winter, the ice breaks up and melt water from the coast increases. All these processes lead to a positive buoyancy flux into the ocean and the restratification of the deep mixed layer, leaving a layer of cold water centered at approximately 100 m called Winter Water (WW). Below WW is a warm and salty water mass called modified Circumpolar Deep Water (mCDW), a slightly colder and fresher version of the oceanic Circumpolar Deep Water (CDW), found along the shelf break of the wAP.

[3] Although precise estimates of the heat and salt budgets of this shelf are lacking, hydrographic surveys and modeling studies suggest that the integrated heat budget for the surface layer results in a net heat loss to the atmosphere [*Smith and Klinck*, 2002]. As heat is readily available from the lower layer on the shelf and mCDW has clearly lost heat after moving onto the shelf, it has been hypothesized that a vertical flux from the lower layer is responsible for balancing the net heat loss to the atmosphere. In turn, an onshore flux of heat must compensate the cooling of the lower layer of the shelf. This flux is thought to come in the form of intrusions of CDW onto the shelf, which also contain high concentrations of nutrients that sustain the rich biological community on the shelf [*Klinck et al.*, 2004; *Hofmann et al.*, 2004]. Hydrographic data from a summer cruise conducted in 1993 suggested that CDW intruded in four specific locations along the shelf break between 64° and 67°S [*Prézelin et al.*, 2000, 2004], which is consistent with previous studies showing similar such intrusions on the shelf [*Domack et al.*, 1992].

[4] A 2-year international field program, the Southern Ocean Global Ecosystem Dynamics (SO GLOBEC), was conducted on the wAP shelf to address fundamental questions about the structure and functioning of the local ecosystem. The hydrography and circulation component of SO GLOBEC set out to investigate the influence of the oceanic water intrusions, the strong seasonal variability of the water column structure, and the main circulation patterns on the shelf, which were hypothesized to contribute to the retention of Krill populations on the shelf [*Hofmann et al.*, 2004].

[5] The observations taken during the field program revealed remnants of CDW along Marguerite Trough (Figure 1) during all of the SO GLOBEC cruises, which also suggested that this bathymetric feature, connecting the shelf break to

[1]Department of Physical Oceanography, Woods Hole Oceanographic Institution, Woods Hole, Massachusetts, USA.
[2]Departamento de Oceanografía, Universidad de Concepción, Concepción, Chile.

0148-0227/09/2008JC004955$09.00

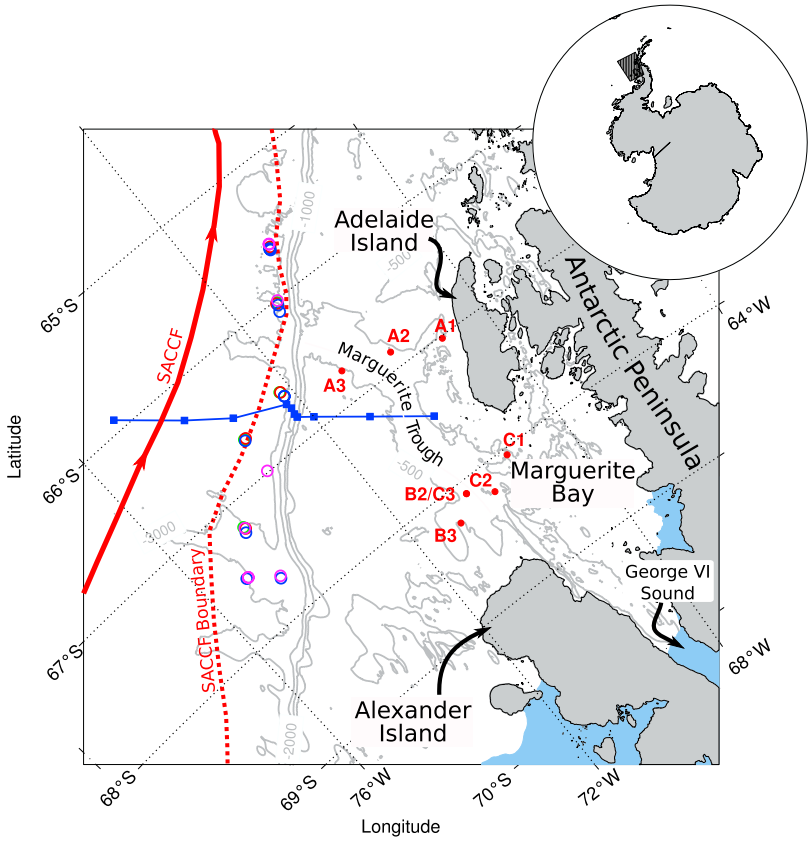

Figure 1. The SO GLOBEC study region. The red lines indicate the location of the Southern Antarctic Circumpolar Current Front (SACCF (solid line)) and its southern boundary (dashed line) from historical data [*Orsi et al.*, 1995]. Also shown are the location of the first ten CTD casts conducted during the S04P cruise (blue squares), the SO GLOBEC moorings (red solid circles), and the CTD stations conducted off the shelf during the SO GLOBEC broad-scale cruises (open circles).

Marguerite Bay, provides a path for CDW intrusions to move across the shelf [*Klinck et al.*, 2004]. On the basis of these hydrographic surveys, it has been hypothesized that CDW moves into Marguerite Trough and across the shelf into Marguerite Bay four to six times a year [*Klinck et al.*, 2004].

[6] In this paper, questions about the spatial scales, frequency and circulation of CDW intrusions onto the shelf are addressed using the SO GLOBEC broad-scale hydrographic cruise and moored array data, which provide the first year-long records of hydrography and circulation on the wAP shelf. In the following sections, we provide a description of the data used, characterization of the source waters for the intrusions, a definition for the intrusions, a characterization of their spatial scales, frequency, intensity and associated circulation. The last two sections discuss the results and provide a summary, respectively.

[7] We will argue that both lower and upper CDW intrude on the shelf and move shoreward along Marguerite Trough, but that the form of the intrusions is rather different for either type, as illustrated in the conceptual diagram shown in Figure 2. Upper CDW (UCDW) intrudes as small and frequent eddy-like features that move onshore and decay away within the midshelf region. In contrast, Lower CDW (LCDW) is found along the bottom of Marguerite Trough (and other deep depressions on the shelf) as a dense layer whose presence is detected throughout the year and has a residence time of approximately six weeks.

2. Data Set

[8] The Southern Ocean Global Ecosystems Dynamics (SO GLOBEC) mooring locations are shown in Figure 1. The 2001–2002 array consisted of one transect (the "A-line") of three moorings (A1–A3) deployed across the shelf west of Adelaide Island and a second transect (the "B-line") of three moorings (B1–B3) deployed west of the mouth of Marguerite Bay. The 2002–2003 array consisted of a L-shaped transect (the "C-line") of three moorings (C1–C3) deployed slightly inshore of the B-line [*Moffat et al.*, 2005]. Table 1 lists the locations, bottom depths and deployment periods of all the moorings.

[9] A2 was located between A1 and A3 on the eastern side of Marguerite Trough, where deep intrusions of UCDW were thought to occur, while A3 was located on the outer shelf in the northeastward flow. The B- and C-lines were deployed across the mouth of Marguerite Bay, although B1 was not recovered. The moorings discussed here were designed to measure (1) temperature at 50, 100, 150, 200, 250, 400 m, and close to the bottom using Sea-Bird Electronics (SBE) temperature sensors; (2) conductivity (salinity) at 50, 100,

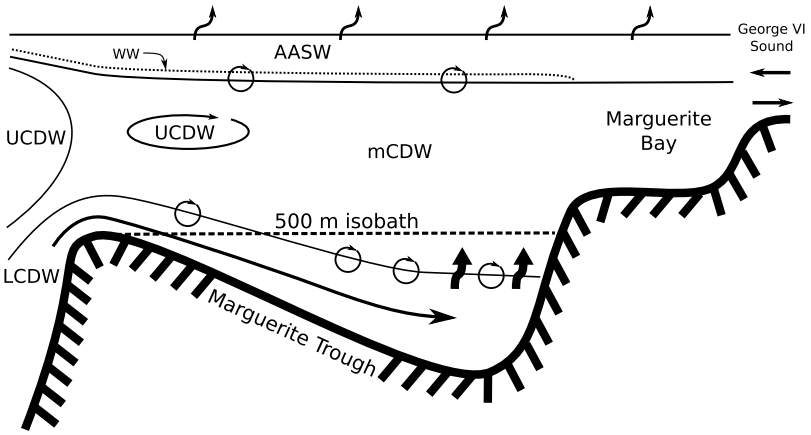

Figure 2. Conceptual diagram showing the characteristics of CDW intrusions to the wAP shelf. UCDW intrudes on the shelf in the form of relatively small and frequent middepth features. LCDW is found at the bottom of Marguerite Trough and other deep depressions. The thick black arrows represent upwelling of LCDW water to the overlying water, and the rounded arrows represent mixing across layers. The circulation and hydrography of Marguerite Bay is also influenced by George VI Sound [*Potter and Paren*, 1985; *Jenkins and Jacobs*, 2008].

250, and 400 m, and close to the bottom using SBE conductivity sensors; and (3) current velocity at 100, 250, and 400 m using Vector Averaging Current Meters (VACMs). A complete description of the moored array data set can be found in the report by *Moffat et al.* [2005].

[10] During 2001 and 2002, four hydrographic cruises were conducted in the study region aboard the RV/IB *N. B. Palmer* (Table 2). These broad-scale cruises provided conductivity-temperature-depth (CTD) (conductivity for salinity, temperature and pressure for depth) profile observations on a grid with a nominal cross-shelf resolution of 20 km. The fall surveys (between May and June) provided a larger spatial coverage than the winter surveys (between August and September), in which weather conditions and sea ice coverage impeded access to Marguerite Bay and other nearshore areas. Details of the processing of the data set can be found in the papers by *Wiebe et al.* [2001] and *Klinck et al.* [2004].

3. Water Mass Structure off the wAP Shelf

[11] A hydrographic section conducted in the austral summer of 1992 along the S04P World Ocean Circulation Experiment line [*Schlitzer*, 2000] illustrates the hydrographic structure of the region. The section was conducted starting near Adelaide Island and moving offshore, with four closely spaced CTD casts across the shelf break (Figure 1). Figure 3 shows the potential temperature (θ), salinity and potential density (σ_θ) sections from the first ten CTD casts conducted during the cruise.

[12] The surface layer is occupied by the relatively fresh and cold AASW. The cold layer found at approximately 100 m corresponds to Winter Water, a remnant of the deep, cold mixed layer formed during the previous winter. Notice the AASW layer tends to be fresher closer to the continent as a result of sea ice melt and fresh water input from the coast [*Jacobs et al.*, 1979; *Sievers and Nowlin*, 1984], and is also typically thicker on the shelf [*Orsi et al.*, 1995]. Away from the shelf and below the AASW, the two types of CDW occupy most of the deep layer. UCDW is characterized by a temperature maximum, an oxygen minimum, and a maximum in nitrate and phosphate concentrations [*Sievers and Nowlin*, 1984]. The colder and saltier water mass below, characterized by a salinity maximum and closely tracked by the 27.8 kg m^{-3} isopycnal, corresponds to LCDW. As is characteristic of the southern boundary of the ACC around Antarctica, both the deep isotherms and isohalines shoal toward the continent [*Sievers and Nowlin*, 1984; *Orsi et al.*, 1995].

[13] Both types of CDW are carried by the Antarctic Circumpolar Current (ACC). The Southern ACC Front, the southernmost of the three ACC fronts (Figure 1), lacks a distinctive surface hydrographic signature [*Orsi et al.*, 1995]. Therefore, we use the local characteristics of CDW off the shelf, instead of surface data, to track the intrusions on the shelf. The SO GLOBEC sampling grid included only a

Table 1. SO GLOBEC Mooring Locations

Mooring	Latitude	Longitude	Bottom Depth (m)	Deployment	Recovery
A1	67°01.134′	69°01.217′	509	26 Mar 2001	13 Feb 2002
A2	66°51.883′	70°00.683′	561	30 Mar 2001	13 Feb 2002
A3	66°45.002′	70°59.991′	487	31 Mar 2001	13 Feb 2002
B1	67°56.890′	69°54.398′	444	30 Mar 2001	Not recovered
B2	68°06.091′	70°31.675′	811	29 Mar 2001	14 Feb 2002
B3	68°15.345′	70°59.853′	447	29 Mar 2001	14 Feb 2002
C1	68°02.940′	69°21.790′	432	18 Feb 2002	22 Feb 2003
C2	68°13.331′	70°01.730′	859	19 Feb 2002	26 Feb 2003
C3	68°06.006′	70°31.799′	811	21 Feb 2002	26 Feb 2003

Table 2. Summary of the Cruise Dates and Number of CTD Stations Conducted

Cruise	Objective	Start	End	Number of CTDs
NBP01-03	Fall 2001 survey	24 Apr 2001	5 Jun 2001	84
NBP01-04	Winter 2001 survey	24 Jul 2001	31 Aug 2001	70
NBP02-02	Fall 2002 survey	9 Apr 2001	21 May 2001	92
NBP02-04	Winter 2002 survey	31 Jul 2002	18 Sep 2002	102

handful of CTD casts in the open ocean during each of the broad-scale surveys, but together they provide a good picture of the variability of the source water for the deep water intrusions. Figure 4 shows a $\theta-$S diagram of all the SO GLOBEC CTD casts collected off the shelf at locations deeper than 2000 m. Unlike the strong seasonal variability observed in the surface layer, the variability below the pycnocline is mostly spatial. Below, we consider the observed properties in order to define an on-shelf intrusion of upper or lower CDW.

3.1. Definition of UCDW Intrusions

[14] The middepth potential temperature maximum corresponding to the core of UCDW (Figure 4 (right)) is characterized by a relatively wide range of potential temperatures (from 1.55 to 2.10°C) and salinities of 34.62 to 34.68, so the potential temperature maximum spans a relatively wide range of isopycnals, as also observed in Drake Passage [*Sievers and Nowlin*, 1984]. In these off-shelf stations, the potential temperature maximum is found at depths ranging from 200 to 550 m. Along the shelf break, this maximum is typically found at shallower depths (less than 430 m), consistent with the observed uplift of isotherms toward the continent (Figure 3).

[15] Although the oxygen minimum has been found to be a more consistent guide to identify UCDW [*Sievers and Nowlin*, 1984], its nonconservative nature makes it a less reliable choice to identify intrusions on the shelf, where strong biological processes are expected. The lack of mooring-based oxygen observations would also limit the analysis to the cruise-based hydrographic data. Moreover, we are ultimately interested in the heat content of these intrusions. The temperature anomalies which accompany any intrusions are, therefore, more relevant for our purposes.

[16] Considering the above, a reasonable detection criteria for UCDW intrusions on the shelf is water warmer than 1.5°C and σ_θ <27.8 kg m^{-3} (see Section 3.2) below the mixed layer. This is consistent with what is known about the source waters carried by the ACC close to the shelf break from observations (Figure 4), and with historical characterizations of the ACC water mass structure and boundaries as seen in Figure 3 and in the literature [*Orsi et al.*, 1995; *Smith et al.*, 1999].

3.2. Definition of LCDW Intrusions

[17] Below UCDW, the $\theta-$S properties tend to tighten (Figure 4) as the salinity increases and temperature decreases. The core of LCDW is characterized, in the SO GLOBEC off-shelf CTD data, by a maximum salinity of around 34.73. The potential temperature for this salinity maximum ranges from 1.25 to 1.57°C, so that temperature alone cannot be used to distinguish UCDW from LCDW (Figure 4). The salinity maximum is found at an average depth of 820 m, but can be found as shallow as 600 m. Unlike UCDW, the salinity maximum is associated with a narrow range of densities, between 27.79 and 27.81 kg m^{-3}. As the deep isopleths bend upward toward the continent, the salinity maximum is found along the shelf break at depths ranging from 500 to 820 m.

[18] With the observed properties off the wAP shelf, we will identify water with potential density >27.8 kg m^{-3} and salinity >34.72 as LCDW intrusions onto the shelf. In the following sections, we use both the SO GLOBEC hydrographic survey and moored array data to look for and characterize UCDW and LCDW intrusions on the wAP shelf.

4. UCDW Events

4.1. Spatial Distribution

[19] Evidence of UCDW on the shelf can be found in the four SO GLOBEC broad-scale cruises. The maximum θ below the mixed layer (Figure 5) shows water of 1.75°C or higher along the shelf break, except for the southern half of the study region during the fall 2001 survey, when no data was collected. The 1.5°C isotherm, representing relatively unmixed UCDW, was found all along the shelf break and on

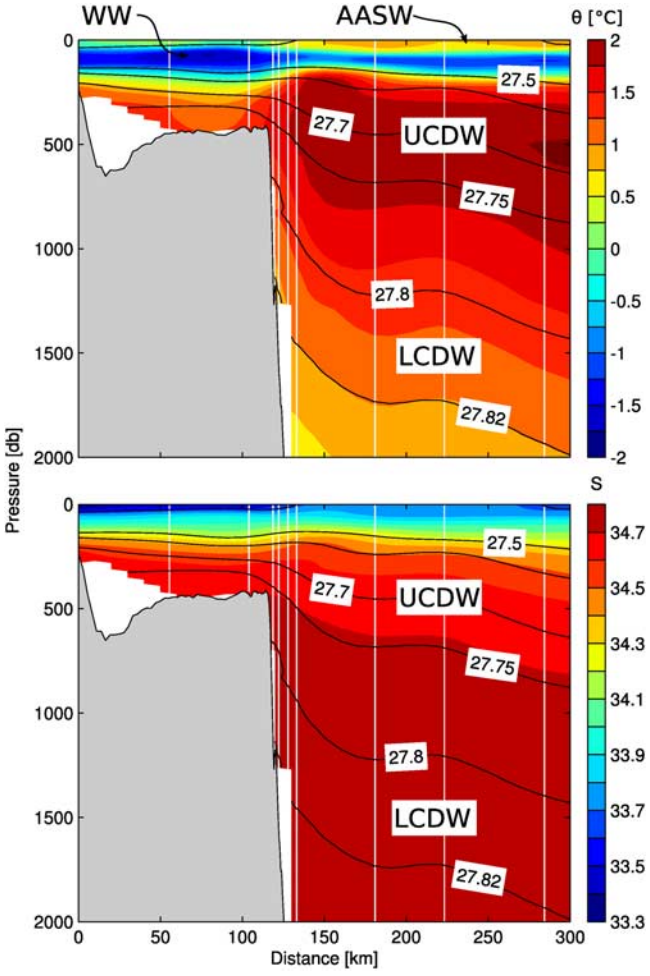

Figure 3. Color contours of (top) potential temperature and (bottom) salinity for the S04P section, conducted between 22 and 24 February 1992. Contours of σ_θ (black) are superimposed. The white vertical lines represent where CTD stations were taken (data from the World Ocean Circulation Experiment database (http://ewoce.org)).

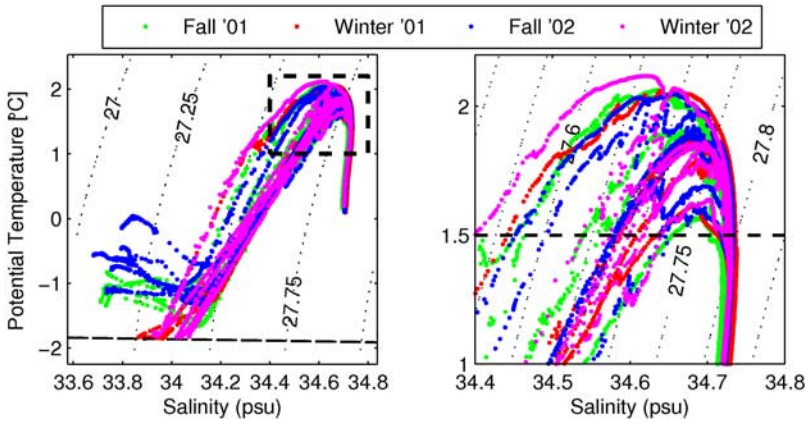

Figure 4. $\theta-$S diagram of all the CTD casts from open ocean locations (>2000 m) collected during fall 2001 (green dots), winter 2001 (red), fall 2002 (blue), and winter 2002 (magenta) SO GLOBEC broad-scale cruises. Locations are shown in Figure 1. (left) The full depth (the dashed line is the freezing temperature) and (right) a detail of the $\theta-$S space associated with CDW (the dashed line marks 1.5°C). Here psu indicates practical salinity units.

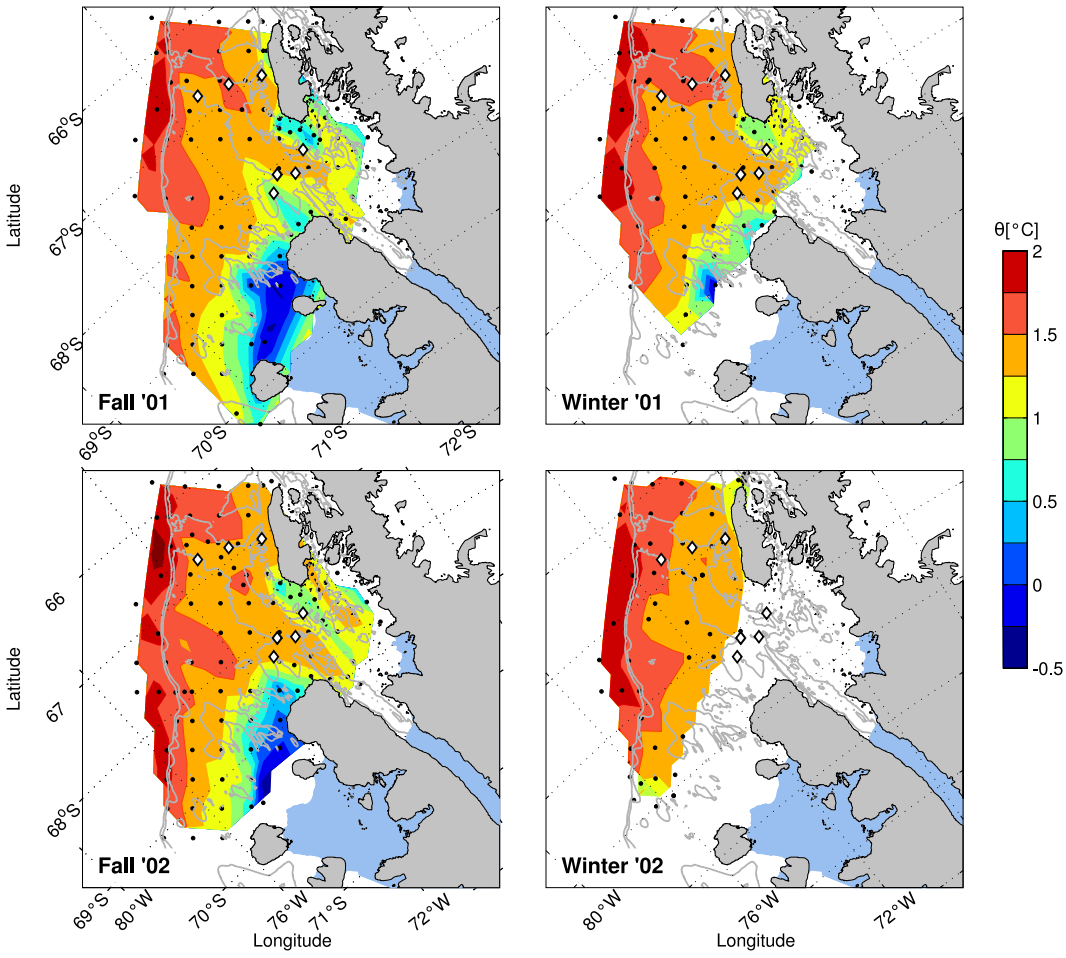

Figure 5. Maximum potential temperature θ below the mixed layer for the four broad-scale SO GLOBEC cruises. The nominal CTD horizontal resolution is 20 km. The isotherms' separation is 0.25°C. Notice Figure 5 is meant to show presence or absence of UCDW (defined here as $\theta \geq 1.5$°C) and should not be interpreted as representing continuous warm intrusions on the shelf (see text for details). The diamonds indicate the location of the SO GLOBEC moorings.

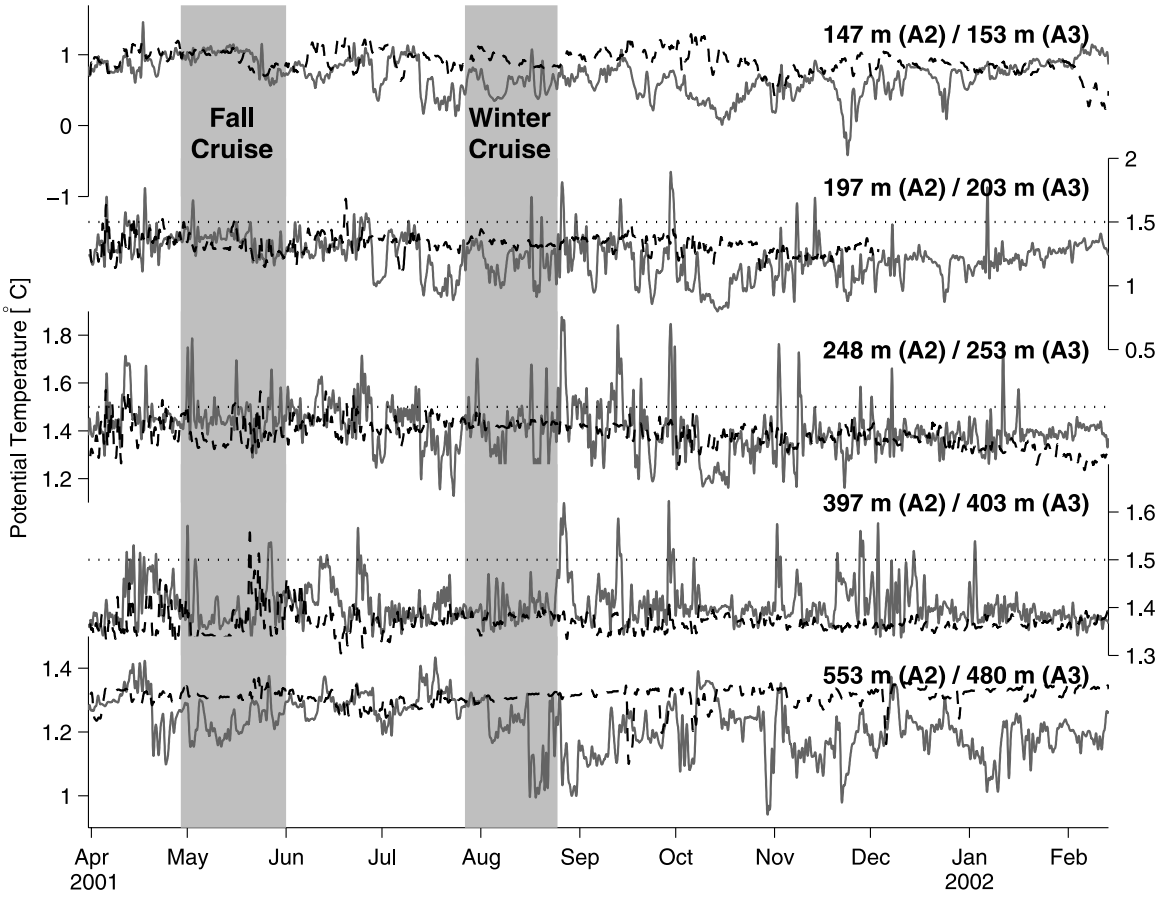

Figure 6. Detided, low-pass filtered time series of potential temperature (θ) at the A2 (solid gray lines) and A3 (dashed black lines) mooring sites. The dotted line indicates 1.5°C.

the outer shelf for all cruises and reaching the midshelf region at two locations: during both fall and winter 2001 surveys and the fall 2002 survey around 67.5°S, and in all of the cruises around 67°S, along the eastern side of Marguerite Trough. Warm water at these two sites was previously observed during hydrographic surveys conducted in 1993 and 1994, which also identified two other intrusion sites to the north of the SO GLOBEC study region [*Prézelin et al.*, 2000, 2004]. These results suggest the presence of large-scale intrusions of UCDW onto the shelf. As we will see below, however, the mooring array data leads to a different conclusion.

[20] The SO GLOBEC moored array (diamonds in Figure 5) is well located to test the hypothesis that Marguerite Trough is one of the locations for UCDW to move across the shelf. The A3 mooring is located 38 km onshore of the shelf break, on the western side of Marguerite Trough (Figure 1). A2 is located 45 km farther onshore (83 km from the shelf break), on the eastern side of the Trough, a location which Figure 5 suggests is a path for the intrusions. The analysis shown below reveals this is indeed the case.

[21] All of the mooring data were first detided using T_TIDE [*Pawlowicz et al.*, 2002] and subsequently low-pass filtered with a 100-weight cosine-lanczos filter with a 20-h half-amplitude period to filter out the inertial frequency variability [*Emery and Thomson*, 2001]. The 20-h half-amplitude is a reasonable compromise between filtering the broad inertial peak centered at 12.9 h while keeping most of the variability associated with the warm water events. All of the records discussed here are for the entire deployment except for the 200-m temperature record at A3, which is 246 days long because the temperature recorder failed on 3 December 2001.

[22] At A2 and A3, water warmer than 1.5°C was detected as intense, high-frequency events in instruments located from 200 m to 400 m (Figure 6). Histograms of potential temperature for the instruments where intrusions were detected (Figure 7) clearly show a higher prevalence of water warmer than 1.5°C at the A2 mooring at all depths. The colder anomalies at A2, particularly at 200 m, are typical of the moorings closer to the coast. At 250 m, where the middepth temperature maximum is usually found on the shelf, temperature higher than 1.5°C was recorded 2% of the time at A3, compared to 15% at A2. At A1, two brief events were recorded at the end of July, when the Antarctic Peninsula Coastal Current (APCC) is absent [*Moffat et al.*, 2008], but the rest of the time series shows no evidence of UCDW. None of the remaining moorings (the B- and C-lines) recorded waters warmer than 1.5°C at depth.

[23] In order to calculate the statistics of the warm events, individual events were defined as follows. For each instrument recording temperature at each mooring, times when the potential temperature was 1.5°C or more were found. The beginning (end) of the event at each depth was defined as the time when the temperature started (finished) increasing

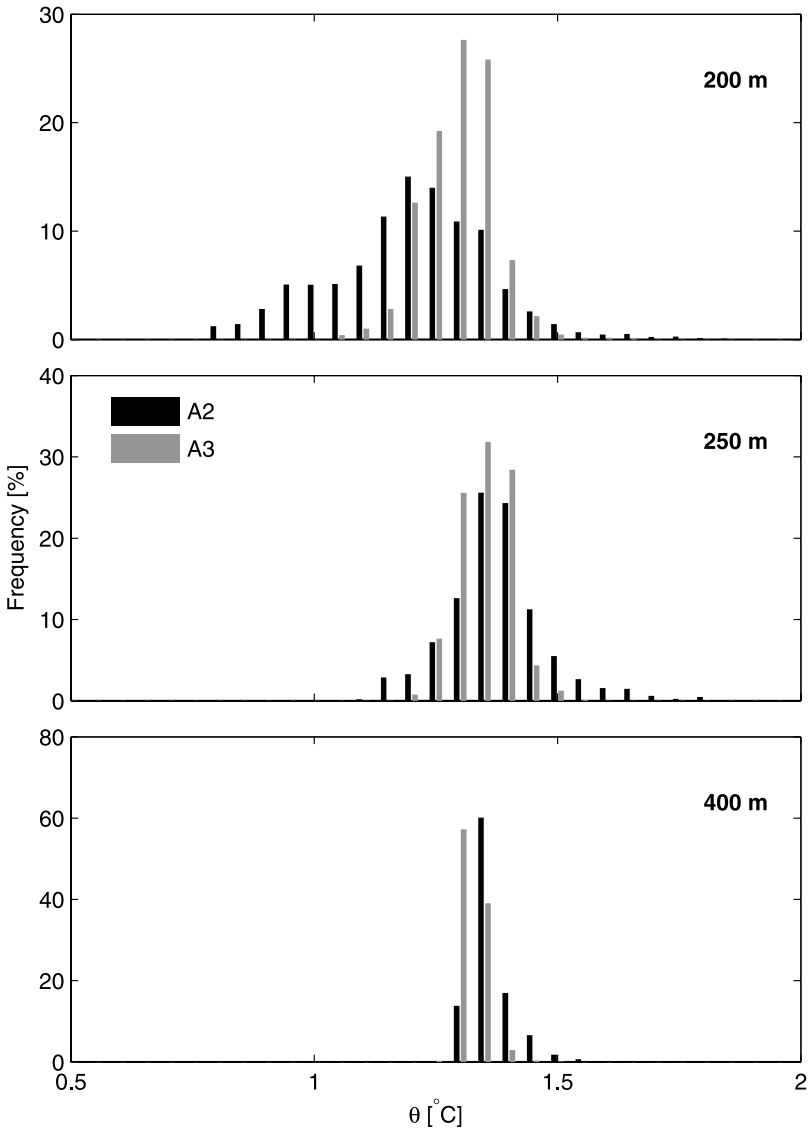

Figure 7. Histogram of potential temperature for the A2 (black) and A3 (gray) moorings at approximately (top) 200 m, (middle) 250 m, and (bottom) 400 m. The 200 m temperature record at A3 is 246 days long (the instrument failed on 3 December 2001), and the rest are ≈318 days long.

(decreasing). If those times overlapped with events recorded at another instrument, it was assumed that they corresponded to one event spanning the entire depth range covered by those instruments.

4.2. Frequency and Duration

[24] Statistics of the events reveal the basic features of the intrusions of UCDW onto the shelf. At A2, 40 events were recorded in the 10.5-month time series, compared to 11 events at A3. At both A2 and A3, the events were relatively short, typically lasting 1 to 3 days, with events as long as 7 days at A2 (Figure 8 (top)). There is no seasonality evident in the occurrence of events. At A2, there are as few as zero events per month (in October) to seven (in May), with an average of four events per month (Figure 8 (bottom)). At A3, all the events occur during the first few months of the deployment, from April to June, resulting in a similar average of events for the fall season as at A2. From July on, no UCDW events were recorded at A3. Moreover, the correlation between the temperature time series at A2 and A3 at depth is not statistically significant, regardless of whether the full time series or the period where intrusions were detected at both sites is considered. However, it must be noted that during the winter 2002 cruise, UCDW was found at the location of the A3 mooring (Figure 5), which suggest that intrusions at this location, although less frequent than at A2, can also occur during different seasons.

4.3. Velocity Structure

[25] The A2 mooring measured currents at 100, 250 and 400 m. There is no clear relationship between the velocity field and the occurrence of warm events. At both moorings, correlations between the horizontal velocity components u or v and θ are small (maximum <0.20 with lags of 1 to 2 days) and statistically not significant at the 95% confidence level. The subtidal current variability has its strongest component in the 5–10 days band and the coherence with temperature oscillations in the 1–3 day band where the intrusions occur

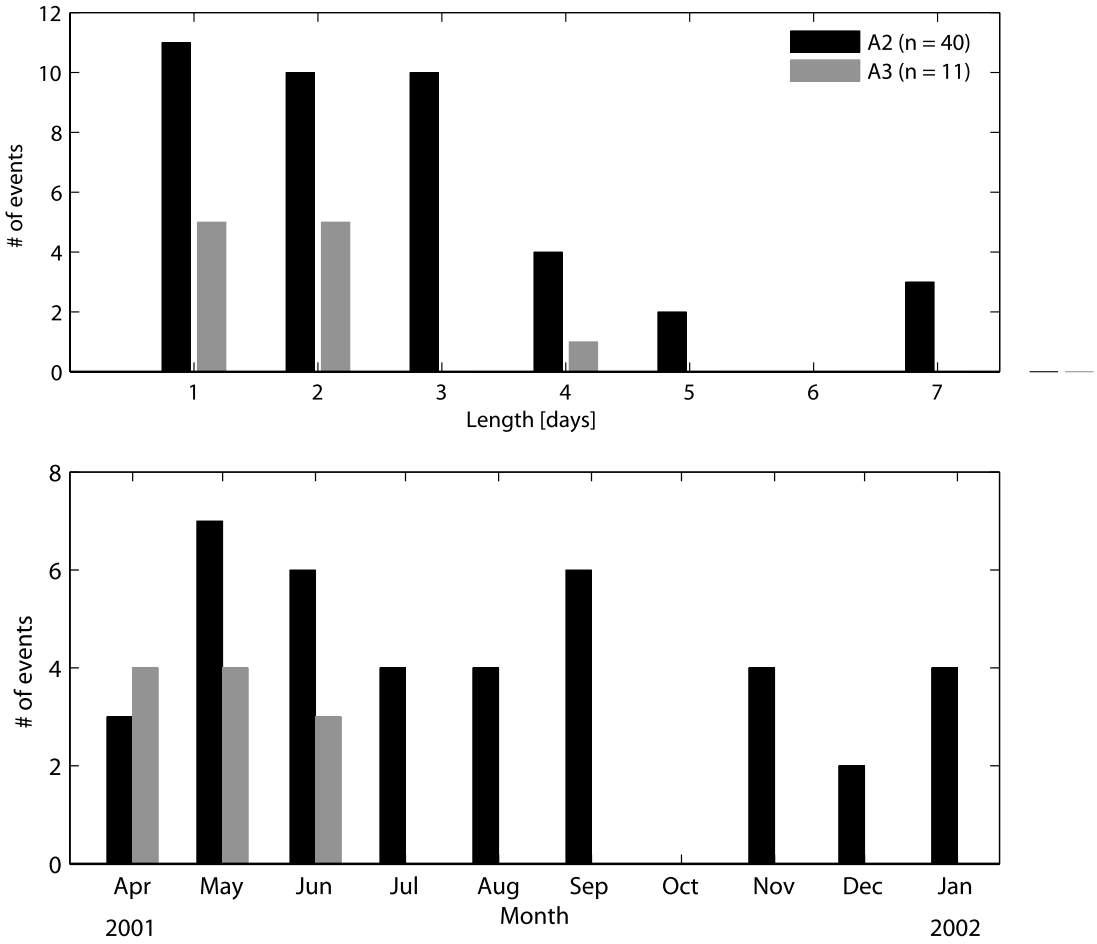

Figure 8. Histogram of the UCDW events' (top) duration and (bottom) number of intrusions per month throughout the 2001/2002 SO GLOBEC mooring deployment (31 March 2001 to 12 February 2002) for the A2 (black, 40 events) and A3 (gray, 11 events) moorings.

is not significant. However, it is important to remember that both cross correlation and coherence analysis average the variability over the entire time series, and might not be appropriate when studying relatively isolated events.

[26] All but three (93%) of the events at A2 have a mean average along-isobath velocity toward the coast, with an overall value of 5.8 ± 2.7 cm s^{-1} (±1 standard deviation). The magnitude and vertical structure of the velocity during the events are very similar to the average structure during the remaining part of the records. The mean velocity during the events has very small vertical shear with a total of 10° counterclockwise veering with depth. For all the intrusions, the flow is dominated by the low-frequency component and the velocities in the ≈3-day frequency band of the UCDW events are typically less than 10% of the low-frequency flow. Overall, this suggests the events are embedded in and advected by a relatively strong low-frequency flow toward the coast.

[27] The moored time series indicate that warm events occur frequently and are short-lived. This is consistent with the survey data (Figure 5) if one considers some important aspects of the survey resolution and the resulting hydrographic fields. First, the warm water found during the survey is associated with different density surfaces at different sites, and therefore the results of Figure 5 should be interpreted as presence of UCDW, not a continuous warm intrusion. Second, the UCDW signal is generally weak when found on the shelf, with temperatures slightly over 1.5°C in thin layers, except for a few CTD casts that show a very strong $\theta-S$ signature. In the fall of 2001, for example, the only station where water warmer than 1.6°C was recorded was located some 20 km from the shelf break on the eastern side of Marguerite Trough. During the winter 2001 cruise, the highest temperature recorded (>1.8°C) on the shelf was also located on the eastern side of the trough, as an isolated patch between the A1 and A2 mooring sites. Another isolated patch of warm water can also be seen in the winter 2002 cruise (Figure 5), as well as in the 1993 survey data (not shown) reported by *Prézelin et al.* [2004]. Third, in the 5 days that it takes to conduct the CTD survey with 20-km horizontal resolution over the northern part of the study region where the warm water was found, one or two distinct events lasting of the order of 1 day each were registered at the A2 mooring. This is inconsistent with the idea of a large-scale intrusion moving onto the shelf, because typical velocities on the shelf are of the order of 5 to 10 cm s^{-1}, which results in an advective timescale of 15 to 30 days for an intrusion moving ≈140 km along Marguerite Trough, as shown in Figure 5.

[28] In summary, it appears UCDW is intruding as frequent, short events, and not as large-scale intrusions. These

events might be instead eddies moving onshore, and leaving, as they mix away on the shelf, the broad regions of weakly elevated temperature observed in the midshelf. In the next section, we explore this hypothesis using a simple model applied to the A2 mooring data.

4.3.1. Eddies Advected Past a Mooring

[29] Let us assume UCDW events are eddies carried by the shelf circulation across the shelf via Marguerite Trough. The horizontal flow as observed by the mooring would be given by:

$$\vec{u} = \vec{U} + \vec{u_e} \tag{1}$$

where $\vec{u}$ is the observed flow, $\vec{U}$ is the background flow, which will be assumed to be spatially uniform but slowly evolving in time, and $\vec{u_e}$ is the flow of the eddy being advected by the background flow past the mooring [*Lilly and Rhines*, 2002]. A sensible option for the eddy flow is given by a Rankine vortex, where the core is in solid body rotation, and outside of which the azimuthal velocity decays with distance from the center of the eddy. In polar coordinates, this velocity is given by

$$v(r) = \begin{cases} VrR^{-1}, & r < R \\ Vr^{-1}R, & r > R \end{cases} \tag{2}$$

where r is the distance from the center of the eddy, V is the maximum azimuthal velocity (at $r = R$), and R is the radius of the eddy. V is taken here to be positive for an anticyclonic eddy.

[30] If UCDW events are eddies being advected past the moorings, one would expect the "cross-stream" velocity, i.e., the component perpendicular to the direction of advection, to have a characteristic signature: early positive (negative) velocities for an anticyclone (cyclone). The eddy flow then becomes

$$\vec{u_e} = (\vec{u} - \vec{U_{lf}})e^{-i\phi(t)} \tag{3}$$

where we take the velocity of the advecting flow U as U_{lf}, the low-pass velocity (5-day half-power Lanczos filter) with direction ϕ. $\vec{u_e} = u_e + iv_e$ is therefore rotated so that v_e is the cross-stream component of the velocity. Any small linear trends remaining in v_e are removed.

[31] There is an important caveat to this analysis: a single mooring recording passing eddies would necessarily tend to underestimate the intensity and size of the eddies since the "sampling" is likely to be off center. Therefore, the average properties over many events are biased and do not represent the true properties of the eddy "population", even under the assumption that A2 is recording all the eddies moving through Marguerite Trough.

4.3.2. Eddy-Like Events in the A2 Records

[32] In order to test the simple model outlined above, the events must be relatively isolated. As described above, the A2 records contain 40 warm events; inspection of the records reveal that most of the longer (>3 days) events appear to be closely spaced short events. As a result, several temperature peaks larger than 1.5°C are evident at each depth in those cases, and individual events are difficult to separate.

[33] For the analysis below, 24 warm events which appear to be reasonably isolated in time were selected. Of those, 19 (79%) had a velocity signature consistent with an anticyclonic eddy, four (17%) with a cyclonic eddy and one was not consistent with either. Examples of a cyclonic and anticyclonic event are shown in Figure 9. Both of them have a strong temperature anomaly at 250 m and a velocity structure spanning the 300-m depth range of the velocity records. The events have scales of 1 day and average cross-stream velocities of 1 to 5 cm s^{-1}.

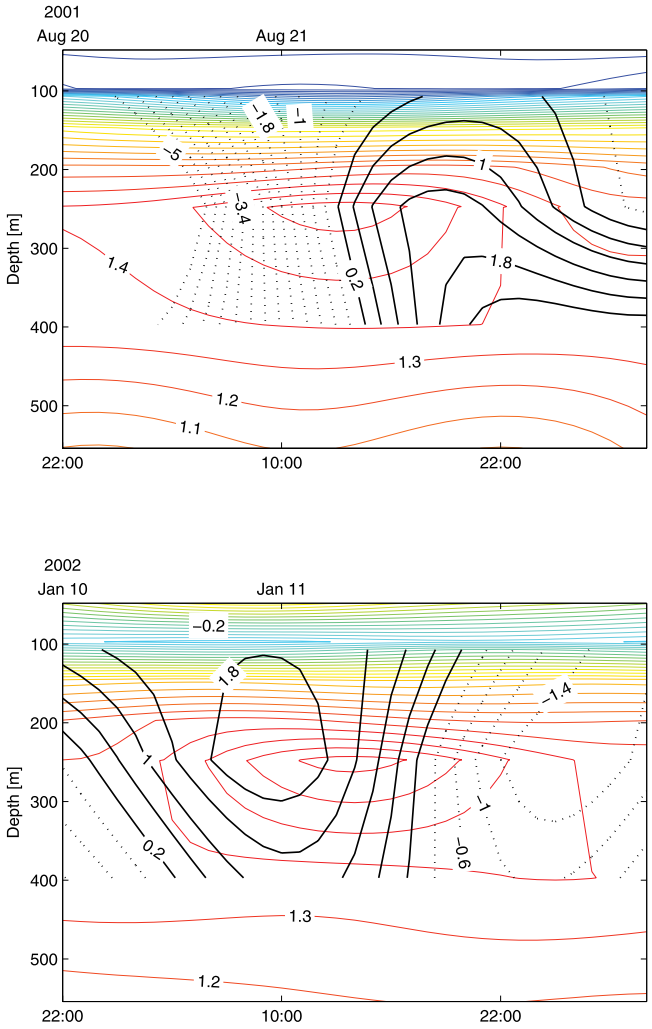

Figure 9. Potential temperature (color contours) and cross-stream (v_e) velocity records (black contours) for (top) a cyclonic and (bottom) an anticyclonic event recorded at A2. Positive (negative) cross-stream velocities are shown as solid (dotted) contours.

[34] Figure 10 shows the potential temperature and velocity records for the 23 events with a consistent "eddy" signature. In order to compare events of different duration, the time coordinate is normalized using the 250-m records, where the temperature signal is strongest, as

$$t' = (t - t_m)/T_{v\max} \tag{4}$$

where t is the time, t_m is the center time between the two absolute maximum v_e during an event (which corresponds to the limits of the eddy chord), and $T_{v\max}$ is the time period between those velocity maximums.

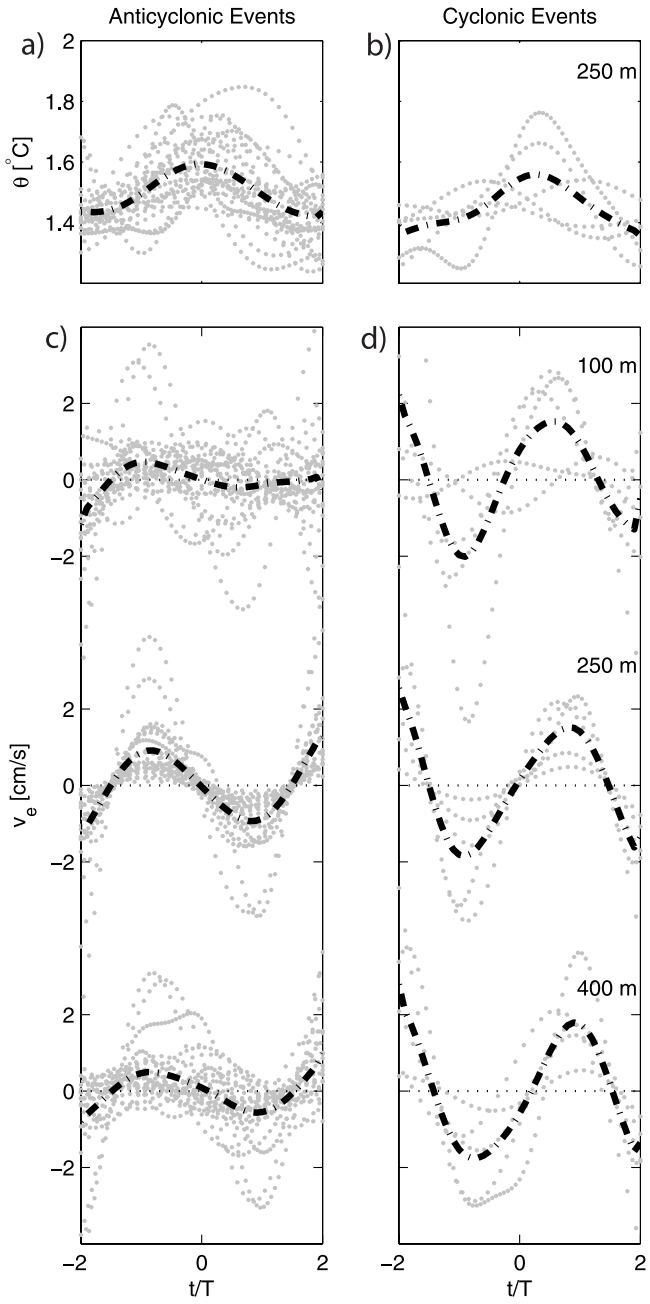

Figure 10. (a, b) Potential temperature at 250 m and (c, d) cross-stream (v_e) velocity records at 100, 250, and 400 m for warm eddy-like events at A2. Fiures 10a and 10c show the anticyclonic events, and Fiures 10b and 10d show the cyclonic events. The gray dots indicate individual records, and the black dashed lines are ensemble averaged for all the events. The time is normalized using equation (4).

[35] On average, the anticyclonic events have a maximum temperature signal of 1.60 ± 0.09°C (±1 standard deviation), with a weak, but consistent, circulation with maximum velocities as large as 4 cm s^{-1} at 250 m but only 0.9 ± 0.7 cm s^{-1} on average. The eddies have, on average, a significant velocity structure at 250 and 400 m, with stronger velocities at mid-depth. The velocity signal at 100 m is not consistent. The cyclonic events have a circulation and temperature signal of comparable magnitude, although because they are rarer their statistics are less certain. Also, notice that the velocity does not tend to diminish at the beginning and end of the period sampled (Figure 10), which is inconsistent with the simple Rankine eddy model used here.

4.4. Events' Intensity and Depth Scale

[36] A measure of the intensity of the eddies can be estimated as

$$\langle \Delta\theta(z) \rangle = \langle \theta_{in}(z) - \theta_{rf}(z) \rangle \tag{5}$$

where θ_{in} is the maximum potential temperature during an event at depth z and θ_{rf} is a profile of reference potential temperature calculated from averages of the time series at times when no intrusions were detected. The brackets indicate an ensemble average of all the events. The same procedure is used to calculate equivalent profiles for salinity ($\langle \Delta S \rangle$) and potential density ($\langle \Delta\sigma_\theta \rangle$). As the reference profile is likely to be influenced by decaying warm events between the region of origin and A2, the values of the intensities discussed here are likely to be lower bounds for the true signal of the events on the shelf.

[37] Figure 11 shows the averaged vertical profiles of $\langle \Delta\theta \rangle$, $\langle \Delta S \rangle$ and $\langle \Delta\sigma_\theta \rangle$ for the same events plotted in Figure 10.

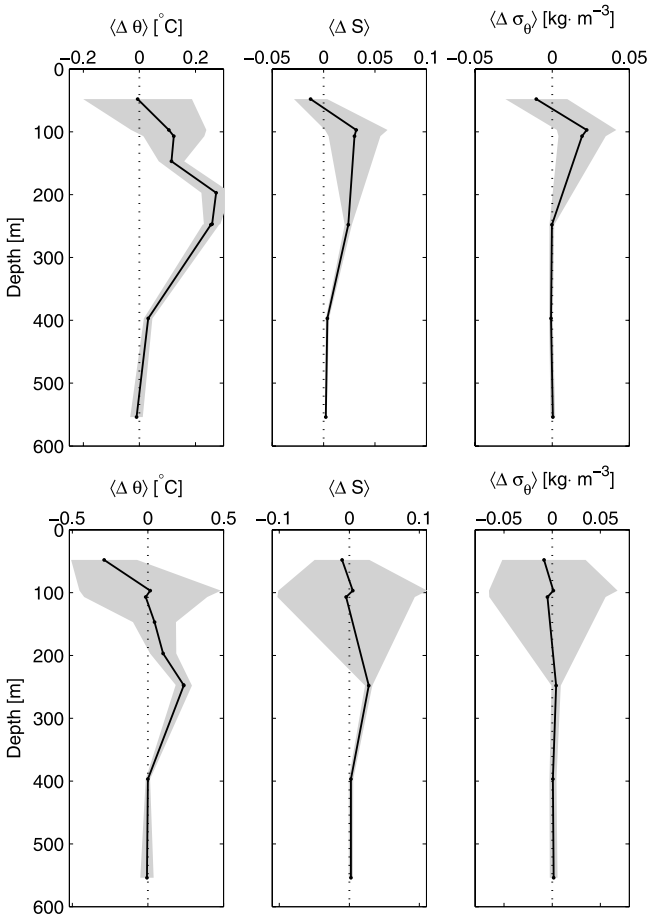

Figure 11. Vertical profiles of $\langle \Delta\theta \rangle$, $\langle \Delta S \rangle$, and $\langle \Delta\sigma_\theta \rangle$ for the A2 mooring corresponding to (top) 19 events identified as anticyclones and (bottom) the 4 events identified as cyclones. The gray shading indicates the 95% confidence interval for the ensemble averages.

On average, the anticyclonic events have a temperature signature at middepth with intensities of 0.26 ± 0.03°C and salinity of 0.030 ± 0.003 at 250 m. Despite having a significant temperature and salinity signature, these warm and salty events have a significant density signal only at 100 m, where the difference is 0.02 ± 0.01. This signature is consistent with the anticyclonic velocity structure shown in Figure 10. The average density at 250 m is roughly 27.75 regardless of the presence of the intrusions.

[38] For the cyclonic events (Figure 11 (bottom)), the hydrographic structure is more ambiguous. They also show a stronger temperature signal at middepth, with the salinity and temperature anomalies nearly compensating. And although the average density signature is negative at 100 m, the variability is large (there are only four events being averaged here), and therefore no firm conclusions can be reached about their vertical structure.

[39] The depth scale of the events is harder to study using the moored array data. In both A2 and A3, there are only a few instruments in the 300-m depth range where UCDW was detected. However, the vast majority of the events were recorded at 250 m in both moorings, with only a handful being detected only at 200 m (2 at A2 and none at A3) or at 400 m (2 at A2 and 1 at A3). Also, 12% of the events (5) at A2 were detected at both 200 m and 400 m. For the events detected by at least two instruments, the results indicate that 20% of the events have a minimum thickness of 150–200 m and a maximum of about 400 m, as the temperature records at 147 m and 554 m at A2 did not register UCDW.

4.5. Horizontal Scale of UCDW Intrusions

[40] An estimate of the horizontal scale of the eddies can be obtained from

$$\langle L \rangle = \left\langle \int_{-T_{v\max}}^{T_{v\max}} U_{lf}\, dt \right\rangle \tag{6}$$

Horizontal scales for the intrusions are roughly 4.2 ± 2.5 km and 4.3 ± 3.5 km for the anticyclonic and cyclonic events, respectively. The internal radius of deformation ($\lambda = NH/f$) below the mixed layer (using $N = 1.3 \times 10^{-3}$ s^{-1}, $H = 400$ m and $f = 1.35 \times 10^{-4}$ s^{-1}) is $\lambda = 3.9$ km. Note that the "sampling" of the eddies by the moorings is biased toward underestimating their size and intensity. Therefore, this estimate appears to be rather reasonable and dynamically consistent with the idea that UCDW events are indeed eddies recorded by the moored array.

5. LCDW Intrusions

5.1. Spatial Distribution of LCDW

[41] Figure 12 shows the near-bottom density for the four broad-scale SO GLOBEC cruises. During all of the cruises, relatively unmixed LCDW, as characterized by water denser than 27.8 kg m^{-3}, is found along the shelf break and on the shelf along Marguerite Trough, reaching as far as the deep (≈1600 m) section of the Trough off the northern tip of Alexander Island and into Marguerite Bay. This dense layer is also found in the deep depression off the northern tip of Adelaide Island and in a few deep depressions near the southern end of the study area.

[42] The structure of LCDW intrusions can be illustrated by a section composed of CTD casts conducted along Marguerite Trough during the winter 2002 cruise (Figure 13). A strong horizontal temperature gradient is evident at the shelf break, which is typical of the boundary of UCDW. A relatively isolated warm patch can be seen at 150 km onshore, which is consistent with the idea that UCDW is found on the midshelf as small, eddy-like blobs.

[43] LCDW, in turn, can be traced by the 27.8 kg m^{-3} isopycnal, which is found at around 900 m depth off the shelf, and on the outer and middle shelf as a layer of the order of 50 to 150 m thick at depths of ≈500 m or more (our data does not show the 27.8 kg m^{-3} isopycnal at depths shallower than 450 m on the shelf). Marguerite Trough deepens relatively gently from the shelf break, where it is roughly 550 m deep, to the mouth of Marguerite Bay, where it reaches approximately 900 m, and then deepens sharply to a maximum depth of 1600 m just off the northern coast of Alexander Island (Figure 1). In this deep depression, the layer with LCDW characteristics is 270 m thick during this cruise, a value consistent with the fall and winter 2001 cruises (280 and 250 m respectively).

[44] The larger average densities within the LCDW layer are found in the outer and middle shelf, and this quantity tends to be at its minimum for the stations collected at the deepest part of the trough, where the layer is relatively homogeneous, with an average density of just over 27.8 kg m^{-3}. This suggests that the observed thickening of the LCDW layer along the Marguerite Trough southward is associated with mixing and entrainment of the overlaying water into the LCDW layer.

[45] Notice, however, that we do not have detailed cross-trough hydrographic sections, and therefore we have assumed that a two-dimensional description is adequate. As the trough (as defined by the 500 m isobath) is roughly 60 km wide near the shelf break and some 12 km at its narrowest, and the internal radius of deformation is of the order of 5 km on the shelf, the LCDW intrusion is very likely to have a significant cross-trough structure.

5.2. Temporal Variability

[46] Examination of the moored array data reveals LCDW is found throughout the year in Marguerite Trough. Figure 14 shows the near-bottom density (7 m above the bottom) for the A- and B-mooring lines. All of the time series show a relatively narrow range of variability (≈0.02 kg m^{-3}). All the A-line moorings show evidence of LCDW. At the A2 mooring site, the deepest of the A-line moorings, the LCDW signal is also the clearest, showing the presence of dense water along the eastern side of Marguerite Trough throughout the deployment. At the A3 mooring site, the record shows consistent presence of LCDW during the first half of the record (until early September), although after that several periods with denser water can be observed, including a few short and intense events (which are uncorrelated with the UCDW events observed in the same mooring). It must be noted that the western side of the trough, where the A3 mooring is located, has a much gentler slope than the eastern side, and the thickness of the LCDW layer from CTD casts there was between 25 to 60 m, thinner than typically found elsewhere in the trough. The A3 record also shows a handful of denser events and little correlation with the variability at

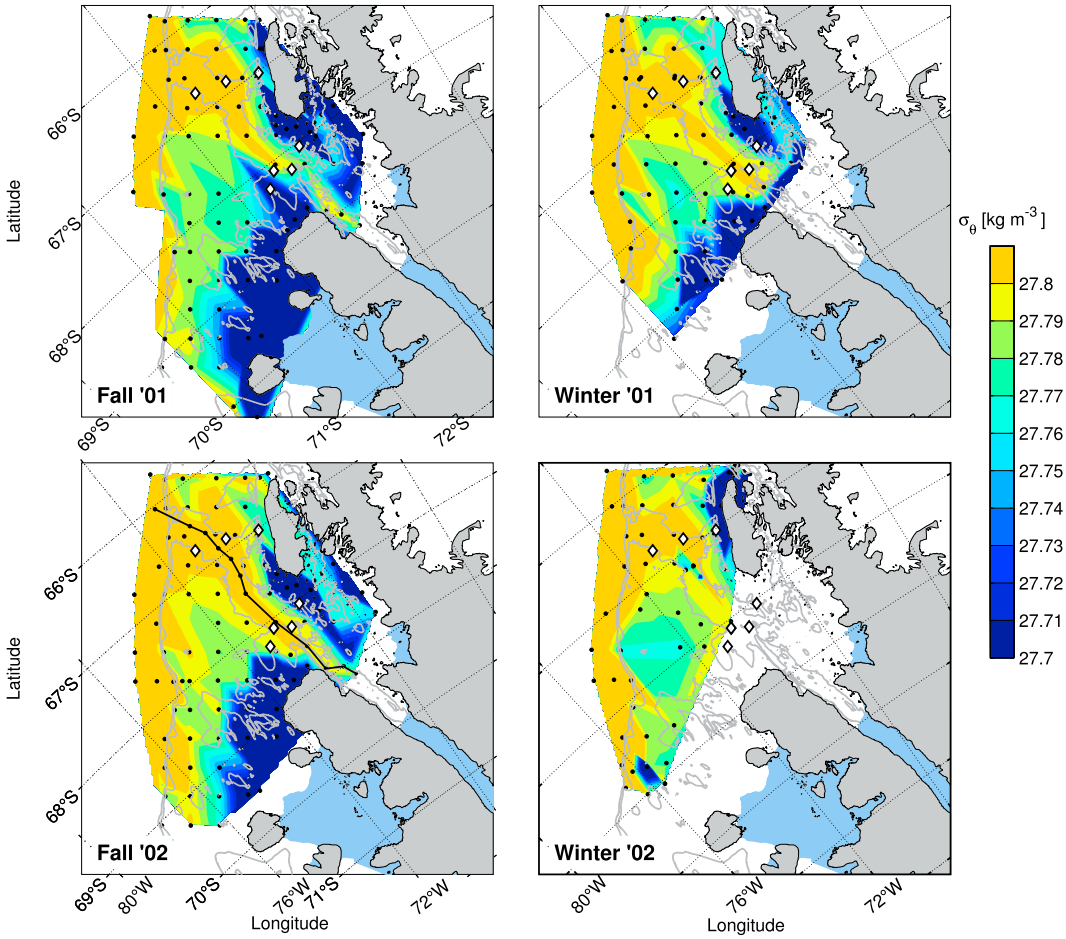

Figure 12. Near-bottom potential density during the broad-scale SO GLOBEC cruises. The nominal CTD horizontal resolution is 20 km. The isopycnal separation is 0.01 kg m^{-3}. The diamonds indicate the location of the SO GLOBEC moorings. The black line in the fall 2002 map indicates the location of the section plotted in Figure 13.

A2, but the presence of LCDW on both moorings, which is consistent with the cruise data, does suggest a relatively broad intrusion, in contrast with the UCDW intrusions discussed earlier.

[47] The A1 mooring site is deep and connected to Marguerite Trough by a channel with a sill depth of 520 m, while the sill depth to the deep depression to the northeast is 370 m. This suggest LCDW is spilling over from Marguerite Trough. Notice that no LCDW is evident at the A1 mooring site in Figure 12 because all the full-depth CTD stations conducted near this mooring were taken at shallower locations around the complicated bathymetry of the site.

[48] Near the mouth of Marguerite Bay, the B2 and B3 moorings show evidence, consistent with the cruise data, that LCDW reaches into the deepest section of Marguerite Trough. The relatively high-frequency variability at B3 is due to a particularly noisy temperature sensor, but it shows a relatively constant density until early June, when it diminishes to ≈27.79 kg m^{-3} for the rest of the record. At B2 the density shows little variability except for a slightly reduced value from mid-June to mid-October.

[49] Although the LCDW intrusions tend to move across the shelf through Marguerite Trough, there is little evidence of correlation with the UCDW events observed in the same locations. This is particularly clear when comparing the density records at A2 (Figure 14) with the potential temperature records at the same mooring (Figure 6). Overall, the data suggest LCDW intruding on the shelf in a few places along the shelf break, but unlike the short, frequent events characteristic of UCDW, LCDW is found in Marguerite Trough throughout the year, penetrating into the shelf farther than UCDW, as far as Marguerite Bay.

6. Discussion

6.1. Horizontal Decay of UCDW Eddies

[50] A main argument presented here is the possibility that the intrusions of UCDW that have been observed on the shelf are a result not of large-scale oscillations of the ACC onto the shelf but instead of small, eddy-like blobs of warm water that are formed either offshore or along the shelf break and move onshore advected by the shelf circulation at certain places, like Marguerite Through. Relatively large structures as observed in Figure 5 could be the result of such eddies mixing away while moving across the shelf. The warm water in the fall of 2001, for example, was detected some 140 km away from the shelf break along Marguerite Trough. The average along-isobath velocity at the A2 mooring is roughly

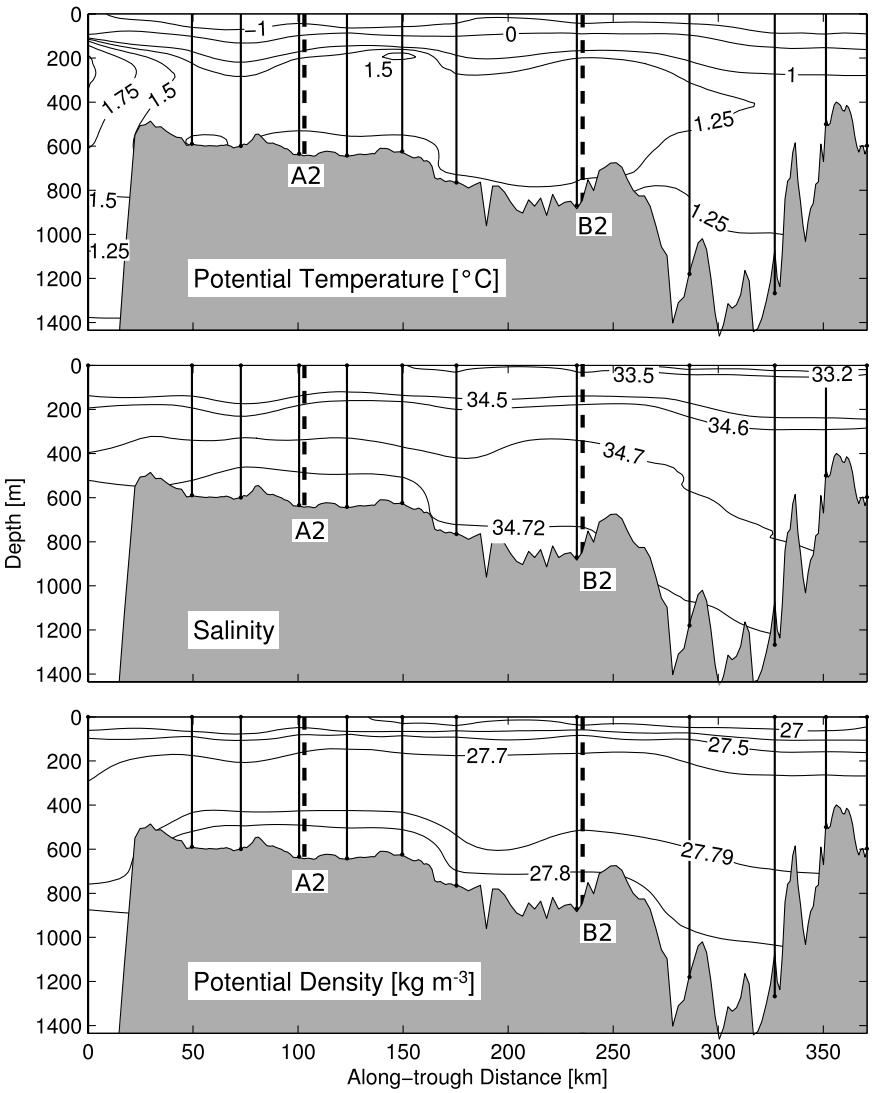

Figure 13. (top) Potential temperature, (middle) salinity, and (bottom) potential density along Marguerite Trough during the winter 2002 broad-scale cruise. The thin vertical lines indicate the location of the CTD casts. The thick dashed vertical lines indicates the approximate location of A2 and B2 moorings along the axis of the trough.

5 cm s^{-1}, which results in an advective timescale T_{adv} of 30 days. An estimate of the frictional spin-down timescale of an eddy is given by *Pedlosky* [1987] as

$$T_{dec} = \frac{D}{(2A_v f)^{1/2}} \tag{7}$$

where D is the vertical scale of the motion and A_v is the vertical eddy diffusivity. A reasonable choice for D is 250 m. Modelling results suggest an A_v of the order of 10^{-4} m^2 s^{-1} is required to close the heat budget on the shelf [*Smith and Klinck*, 2002], although the limited available observations suggest values of the order of 10^{-5} m^2 s^{-1} at the pycnocline [*Howard et al.*, 2004]. This latter value was calculated using shear measurements during relatively calm atmospheric conditions and it probably does not reflect the diffusivity values found during the strong storms common in this area [*Howard et al.*, 2004]. With this order-of-magnitude range for the diffusivity, the decay timescale T_{dec} is between 17 and 55 days. This suggests that if this mechanism explains the decay of the eddies, a higher average diffusivity than measured so far is required for the eddies to decay in the midshelf region. This would be consistent with the absence of unmixed UCDW in Marguerite Bay and the diffusivity estimates from numerical models.

6.2. Mixing of LCDW Water

[51] The structure of the LCDW intrusion across the shelf raises an interesting question about its fate on the shelf. As the trough deepens toward the coast, the top of the LCDW layer is quickly found below what can be reasonably thought as the rim of the trough, which we will take here to be 500 m. The LCDW layer is bounded by the trough and there is no indication of any way for this layer to be drained except through mixing with the overlying water. Assuming this deep reservoir of LCDW is only fed by the intrusions described in Section 5, a possible steady state for the deep section of the

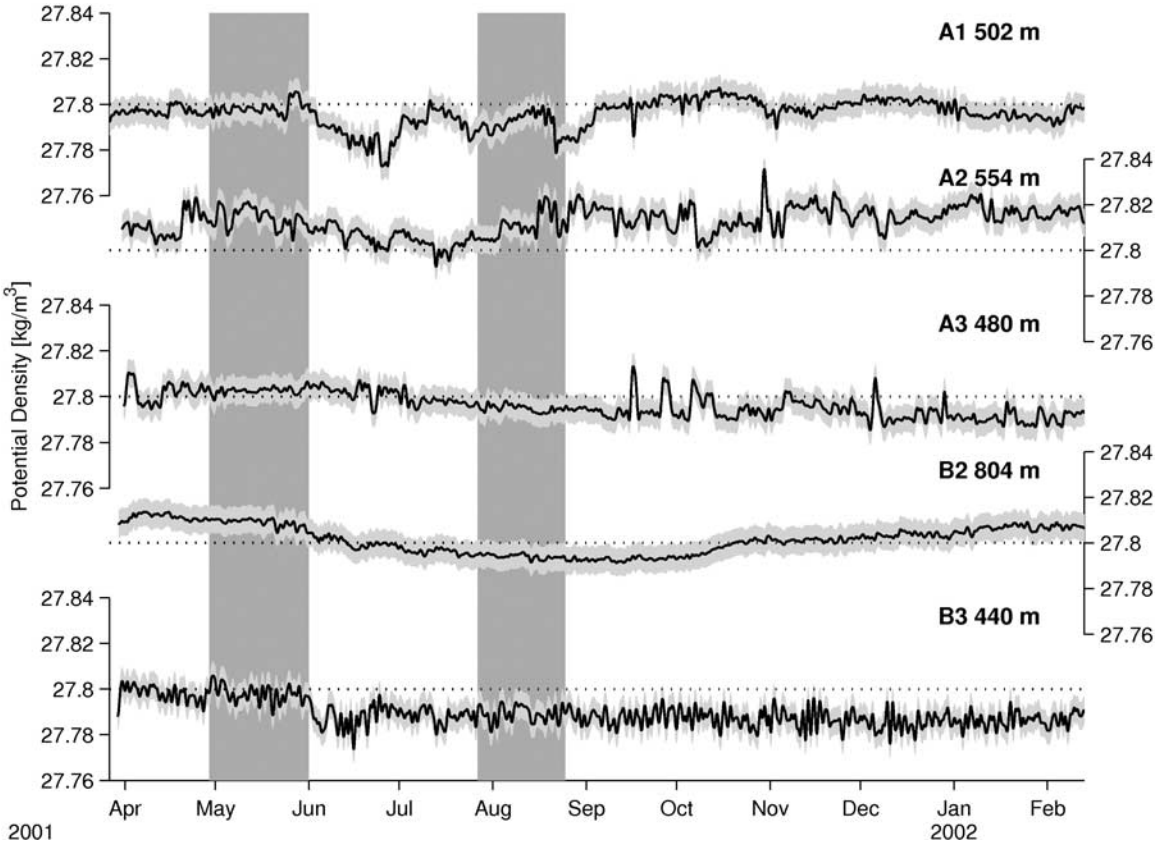

Figure 14. Detided, low-pass filtered time series of potential density (σ_θ) from the near-bottom instruments at each of the moorings from the 2001 moored deployment. All of the instruments were located at a nominal depth of 7 m above the bottom. The dotted line indicates 27.8 kg m^{-3}.

trough is given by the advective-diffusive balance [*Morris et al.*, 2001]:

$$\int_v \nabla \cdot (\mathbf{u}\sigma_\theta) dV = \int_v (\kappa \sigma_{\theta z})_z dV \tag{8}$$

where $\mathbf{u}$ is the three-dimensional flow field and σ_θ is the density field. The above equation can be integrated over a volume bounded by the 27.8 isopycnal, from the location of the A2 mooring onshore:

$$U\sigma_\theta^{in} + W\sigma_\theta^{top} = [\overline{\kappa\sigma_{\theta z}} A]^{top} \tag{9}$$

where U is the volume transport into the trough with transport-weighted density σ_θ^{in}, W is the volume transport through the top of the volume with density σ_θ^{top} (27.8 kg m^{-3}). These advective fluxes are balanced by vertical mixing of buoyancy with a eddy diffusivity κ over an area A. Mass conservation requires U and W to balance, and by further assuming $\overline{\kappa\sigma\theta_z} \approx \bar{\kappa}\overline{\sigma\theta_z}$, we can estimate the eddy diffusivity as

$$\bar{\kappa} = \frac{U\delta\sigma_\theta}{\overline{\sigma_{\theta z}} A} \tag{10}$$

where $\delta\sigma_\theta = \sigma_\theta^{in} - \sigma_\theta^{top}$. The volume transport U is estimated from extrapolating the average velocity at 400 m at the A2 mooring (and thus assuming the flow is basically barotropic below this level), with uncertainty defined as the standard error of the velocity records and an additional 50% added to account for unknown variations of the velocity below 400 m and across the trough. The LCDW layer is estimated to be approximately 75 m thick at the A2 location, where the trough is ≈41 km wide. This estimate is consistent from the data shown in Figure 13 and from finding the depth of the 27.8 kg m^{-3} isopycnal from linear interpolation of the mean density profile of the A2 mooring data. The average density of the inflow σ_θ^{in} is also estimated from the mooring data by assuming the above mentioned thickness (75 m) and mapping the mean density profile from the A2 mooring data to this layer using the density records at 400 and 554 m. $\delta\sigma_\theta$ is assumed to have a 50% uncertainty. The other variables are estimated using the hydrographic data shown in Figure 13. The area A is estimated using the depth of the LCDW layer, which is assumed independent of the cross-trough direction. A 25% uncertainty is assigned to this quantity to account for uncertainties in the height of the isopycnal of interest. The average vertical density gradient $\overline{\sigma\theta_z}$ on A is calculated by a linear fit of the density profiles shoreward of A2 (Figure 13) across a layer 40 m thick centered at the depth of the 27.8 kg m^{-3} isopycnal (using all the data available within the trough does not change this estimate significantly). The uncertainty of this quantity is obtained from an error estimate of the linear fit and an additional 50% uncertainty.

[52] The estimates of U ($2.01 \pm 0.02 \times 10^5$ m^3 s^{-1}), A ($6.3 \pm 1.6 \times 10^9$ m^2), $\delta\sigma_\theta$ ($6 \pm 3 \times 10^{-3}$ kg m^{-3}) and $\overline{\sigma\theta_z}$ ($1.38 \pm 0.02 \times 10^{-4}$ kg m^{-3}) result in an average upwelling rate of $3.2 \pm 0.8 \times 10^{-5}$ m s^{-1}. At this rate, the residence time of the LCDW layer is roughly 40 days. Using all of the above values, the estimated average diffusivity is $\overline{\kappa} = 1.4 \pm 0.8 \times 10^{-3}$ m^2 s^{-1}. There are no published estimates for the diffusivity in the deep layer (>500 m) of concern here, although studies attempting to estimate the heat fluxes across the pycnocline have found lower values, of the order of 10^{-5} m^2 s^{-1} [*Howard et al.*, 2004], but it is unclear at this point whether this and other studies [*Smith and Klinck*, 2002] are relevant for the mixing of LCDW. The problem of how large a buoyancy flux through the pycnocline (and by extension, laterally into the lower layer) and how large are the necessary diffusivities remain unresolved because of the lack of observations of at least two possible sources of mixing on the shelf: spatially localized mixing associated with the complicated bathymetry or nearshore processes [*Dorland and Zhou*, 2008; *Jenkins and Jacobs*, 2008] or intermittently high mixing associated with strong storms. More detailed observations of the mixing processes on the shelf are required to resolve this issue.

7. Conclusions and Summary

[53] Here we have characterized intrusions of both types of CDW onto the wAP shelf, which are thought to strongly influence the hydrographic structure on the shelf. A number of conclusions can be drawn from this work.

[54] First, the analysis presented here suggests that Marguerite Trough, and in particular its eastern side, is a path for warm UCDW water to move across the shelf. Almost four times as many UCDW events were recorded on the eastern side of Marguerite Trough (at A2) compared to the western side (at A3).

[55] Second, UCDW events are much smaller in scale and more frequent than had been inferred from broad-scale hydrographic surveys. The sampling bias introduced by the 20-km CTD cast separation typical of the SO GLOBEC and other seasonal surveys in this area had suggested that intrusions had large horizontal scales significantly larger than the internal radius of deformation and with a frequency of roughly six per year. The results presented here suggest otherwise. The UCDW intrusions have a maximum thickness of a few hundred meters, and they occur roughly four times a month on average. A simple model of an isolated eddy being advected past a mooring was shown to be somewhat consistent with the observations at A2, and results in eddies with an horizontal scale of 4 to 5 km and associated currents of 1 to 2 cm s^{-1}.

[56] Although this work does not attempt to answer questions about the formation process of the intrusions, it does help to provide some constraints for their spatial and temporal scales. This has straightforward implications for the wAP ecosystem. *Prézelin et al.* [2000] noted that diatom populations on the middle and outer shelf depend on the renewal of the silica-rich UCDW. The work presented here suggests that this renewal is frequent and more or less continuous throughout the year, which has important implications for the continuous success of the biological community.

[57] Third, LCDW is found in several deep locations on the shelf, but as UCDW, it is consistently found along Marguerite Trough. LCDW is found as a tongue of dense water at depths of 450 m or more which tends to thicken as the trough deepens toward the coast. An order-of-magnitude calculation of the necessary mixing to maintain the observed vertical structure resulting from LCDW intrusions using a simple advective-diffusive balance is presented. This calculation suggest the LCDW layer is renewed every 40 days or so and that the average diffusivity is $\overline{\kappa} = 1.4 \pm 0.8 \times 10^{-3}$ m^2 s^{-1}. However, it must be noted that this is a poorly constrained calculation and that further observations and analysis are required to test its validity.

[58] An important lesson from this study is that in order to both test some of the ideas presented here and respond to some of the many open questions remaining, observations that can resolve horizontal distances of 1 to 2 km and timescales of the order of 1 day need to be collected in this region, particularly along Marguerite Trough.

[59] **Acknowledgments.** We want to thank the crew of the research vessels *L. M. Gould* and *N. B. Palmer* for their help in the collection of the data used here. We also want to thank Richard Limeburner (WHOI) and Scott Worrilow (WHOI) and his crew in the Subsurface Mooring Operations Group and the Rigging Shop at WHOI for the successful deployment and recovery of the moored array and the preliminary data processing. John Klinck (Old Dominion University) provided the hydrographic data. Steve Lentz and Ken Brink (WHOI) and Glen Flierl (MIT) provided valuable comments to an early version of this paper. Two anonymous reviewers offered thoughtful criticism and suggestions for improvements to this paper. This work was supported by the National Science Foundation Office of Polar programs through U.S. Southern Ocean GLOBEC grants OPP 99-10092 and 06-23223. C. Moffat also received support from the Chilean government through its Presidential Fellowship program and the Coastal Ocean Institute at WHOI and the Cooperative Institute for Climate and Ocean Research at WHOI. This is U.S. GLOBEC contribution 639.

References

Domack, E., E. Schere, C. McClennen, and J. Anderson (1992), Intrusion of Circumpolar Deep Water along the Bellingshausen Sea continental shelf, *Antarct. J. U. S.*, *27*, 71.

Dorland, R., and M. Zhou (2008), Circulation and heat fluxes during the austral fall in George VI Sound, Antarctic Peninsula, *Deep Sea Res., Part II*, *55*, 294–308.

Emery, W., and R. Thomson (2001), *Data Analysis Methods in Physical Oceanography*, 2nd ed., Elsevier Sci., San Diego, Calif.

Hofmann, E. E., P. Wiebe, D. P. Costa, and J. J. Torres (2004), An overview of the southern ocean global ocean ecosystems dynamics program, *Deep Sea Res., Part II*, *51*, 1921–1924, doi:10.1016/j.dsr2.2004.08.007.

Howard, S., J. Hyatt, and L. Padman (2004), Mixing in the pycnocline over the western Antarctic Peninsula shelf during Southern Ocean GLOBEC, *Deep Sea Res., Part II*, *51*, 1965–1979.

Jacobs, S., A. Gordon, and A. Amos (1979), Effect of glacial ice melting on the Antarctic surface water, *Nature*, *277*, 469–471.

Jenkins, A., and S. Jacobs (2008), Circulation and melting beneath George VI ice shelf, Antarctica, *J. Geophys. Res.*, *113*, C04013, doi:10.1029/2007JC004449.

Klinck, J. M., E. E. Hofmann, R. C. Beardsley, B. Salihoglu, and S. Howard (2004), Water-mass properties and circulation on the west Antarctic peninsula continental shelf in austral fall and winter 2001, *Deep Sea Res., Part II*, *51*, 1925–1946.

Lilly, J., and P. Rhines (2002), Coherent eddies in the Labrador Sea observed from a mooring, *J. Phys. Oceanogr.*, *32*, 585–598.

Moffat, C., R. Beardsley, R. Limeburner, W. Owens, M. Caruso, and J. Hyatt (2005), Southern ocean globec moored array and automated weather station data report, *Tech. Rep. WHOI-2005-07*, Woods Hole Oceanogr. Inst., Woods Hole, Mass.

Moffat, C., R. C. Beardsley, B. Owens, and N. van Lipzig (2008), A first description of the Antarctic Peninsula Coastal Current, *Deep Sea Res., Part II*, *55*, 277–293.

Morris, M., M. Hall, and N. Hogg (2001), Abyssal mixing in the Brazil Basin, *J. Phys. Oceanogr.*, *31*, 3331–3348.

Orsi, A., T. Whitworth, and W. Nowlin (1995), On the meridional extent and fronts of the Antarctic Circumpolar Current, *Deep Sea Res., Part I*, *42*, 641–673.

Pawlowicz, R., R. Beardsley, and S. Lentz (2002), Classical tidal harmonic analysis including error estimates in MATLAB using T_TIDE, *Comput. Geosci.*, *28*, 929–937.

Pedlosky, J. (1987), *Geophysical Fluid Dynamics*, 2nd ed., Springer, New York.

Potter, J., and J. Paren (1985), Interaction between ice shelf and ocean in George VI Sound, Antarctica, in *Oceanology of the Antarctic Continental Shelf*, *Antarct. Res. Ser.*, vol. 43, edited by S. Jacobs, pp. 35–58, AGU, Washington, D. C.

Prézelin, B., E. Hofmann, C. Mengelt, and J. Klinck (2000), The linkage between upper Circumpolar Deep Water (UCDW) and phytoplankton assemblages on the west Antarctic Peninsula Continental Shelf, *J. Mar. Res.*, *58*, 165–202.

Prézelin, B., E. Hofmann, M. Moline, and J. Klinck (2004), Physical forcing of phytoplankton community structure and primary production in continental shelf waters of the Western Antarctic Peninsula, *J. Mar. Res.*, *62*, 419–460.

Schlitzer, R. (2000), Electronic atlas of WOCE hydrographic tracer data now available, *Eos Trans. AGU*, *81*(5), 45.

Sievers, H., and W. Nowlin (1984), The stratification and water masses at Drake Passage, *J. Geophys. Res.*, *89*, 10,489–10,514.

Smith, D., and J. Klinck (2002), Water properties on the west Antarctic Peninsula Continental Shelf: A model study of effects of surface fluxes and sea ice, *Deep Sea Res., Part II*, *49*, 4863–4886.

Smith, D. A., E. Hofmann, J. Klinck, and C. Lascara (1999), Hydrography and circulation of the west Antarctic Peninsula Continental Shelf, *Deep Sea Res., Part I*, *46*, 925–949.

Wiebe, P., et al. (2001), Report of RV/IB *Nathaniel B. Palmer* cruise 01-03 to the western Antarctic peninsula 24 April to 5 June 2001, *Tech. Rep. 2*, U.S. South. Ocean Global Ocean Ecosystems Dyn. Program.

R. C. Beardsley, C. Moffat, and B. Owens, Department of Physical Oceanography, Woods Hole Oceanographic Institution, Mail Stop 21, 266 Woods Hole Road, Woods Hole, MA 02543, USA. (cmoffat@whoi.edu)